

# MICROSCOPE SYSTEM WITH ON AXIS PROGRAMMABLE FOURIER TRANSFORM FILTERING

José Luis Martínez<sup>1</sup>, Pascuala García-Martínez<sup>2,\*</sup>, Ignacio Moreno<sup>1</sup>

1. Departamento de Ciencia de Materiales, Óptica y Tecnología Electrónica, Universidad Miguel Hernández de Elche, 03202 Elche, Spain

2. Departamento de Óptica, Universidad de Valencia, 45100 Burjassot, Valencia, Spain

## Abstract

We propose an on-axis microscope optical system to implement programmable optical Fourier transform image processing operations, taking advantage of phase and polarization modulation of a liquid crystal on silicon (LCOS) display. We use a Hamamatsu spatial light modulator (SLM), free of flickering, which therefore can be tuned to fully eliminate the zero order component of the encoded diffractive filter. This allows the realization of filtering operation on axis (as opposed to other systems in the literature that require operating off axis), therefore making use of the full space bandwidth provided by the SLM. The system is first demonstrated by implementing different optical processing operations based on phase-only blazed gratings such as phase contrast, band-pass filtering, or additive and subtractive imaging. Then, a simple Differential Interference Contrast (DIC) imaging is obtained changing to a polarization modulation scheme, achieved simply by selecting a different incident state of polarization on the incident beam.

\* Corresponding Author: [Pascuala.Garcia@uv.es](mailto:Pascuala.Garcia@uv.es)

**Keywords:** Spatial Light Modulator (SLM), Liquid Crystal on Silicon (LCOS), optical microscopy, blazed gratings, phase and polarization modulation, Differential Interference Contrast (DIC).

## 1. INTRODUCTION

Spatial light modulators (SLM) are currently used in various applications in optical microscopy, including the generation of an array of optical beams [1], the production of optical traps [2], photo-stimulation [3], the synthesis of arbitrary point spread functions [4], or quantitative phase microscopy [5]. One of the most promising methods is the use of liquid crystal displays (LCD) as programmable phase diffractive optical elements (DOE) placed in the Fourier plane giving access to the spatial frequencies, which can be phased shifted individually, allowing to emulate a wealth of contrast enhancing methods [6,7]. Some of those DOE elements are spiral phase patterns [8,9] giving a strong contrast enhancement of microscopic amplitude and phase samples [10], or phase masks as circular rings or annular structures [11].

In these cases, blazed gratings are displayed on the SLM acting as phase masks that diffract the incoming wave into the first diffraction order image plane [5,6,12,13]. This is mainly due to the SLM flicker effect, that causes a temporal fluctuation of the phase values displayed on the SLM, and is the origin of some important amount of undiffracted intensity [14,15]. So, for such systems it is needed to block the zero-order, and to operate with an off-axis architecture. This operation with a blazed grating reduces substantially the available space bandwidth provided by the SLM. Although a better control of the spatial phase and amplitude modulation of the diffracted beams are a justification to use those systems, what it is true is that off-axis systems have a relevant reduction of light and field of view, as well as some difficulties of stability and optical implementation.

In this work, instead, we use a parallel-aligned Hamamatsu LCOS display, PAL-LCOS-SLM model X10468-01 [16]. Although these LCOS devices suffer from other typical problems of LCOS SLMs like non-uniformities, fringing effects or Fabry-Perot effects [17], they are free of flicker and therefore they can completely eliminate the zero order component of blazed phase diffractive elements, when operated correctly. Therefore, the purpose of this paper is to describe a programmable microscope system where such an LCOS SLM is employed to display Fourier transform filters, with the advantage of operating on axis. We demonstrate this ability by applying some simple pass band filtering operations, as well as some polarization filtering.

Various imaging-based measurement techniques are capable of delivering information in the form of phase, where phase imaging methods and polarized microscopy are used to extract anisotropy or birefringence information. In fact birefringence characterized the differential speed of propagation between two orthogonal polarization states. Several techniques for determining the optical birefringence have been used, including interferometric [18] and polarimetric methods [19,20]. Polarized microscopy is based on optical microscopy techniques involving polarized light. A more complex microscopy techniques which take advantage of polarized light include differential interference contrast microscopy (DIC) [21]. DIC works on the principle of interferometry to gain information about the optical path length of the sample, to see otherwise invisible features. Traditionally it is performed using Wollaston prisms to create two slightly offset coherent images that are superimposed in the image plane [21,22]. DIC has been used satisfactorily with SLM [12,23] where Wollaston prism are replaced by a SLM to generate and overlap the two displaced images without taking advantage of the polarization orthogonality of the anisotropy of the LC. In previous methods the shear, orientation and phase difference of the images are all computer controlled and can be varied at video rates. The requirement of computer processing is not always an advantage since the illumination conditions and alignment is critical to perform the correct digital image addition.

In this work we propose the on-axis microscope set-up to implement optical image processing operations by exploiting the phase and polarization properties of the LCOS display. The optical system is equivalent to other typical previous architectures [6,7,12,13,23] where a LC SLM is used as spatial filter in a Fourier plane that is made available by means of a relay optics. There, a phase or polarization filter is displayed, but no zero-order component is obtained. We then use a beam splitter (BS) to recover the information that come from the Fourier plane and recombining it in the final image plane, where a CCD camera is placed. By selecting the proper linear polarization impinging to the LCOS SLM different parallel basic image processing operations are done. In addition we propose a simple architecture to perform DIC microscopy without need to computer processing. We use the polarization properties of the LCD by placing a polarizer oriented 45° angle with respect the two orthogonal polarizations. So the two slightly offset coherent images are superimposed in the final image plane. This is the fundamental work of DIC by separating a polarized light source into two orthogonally polarized mutually coherent parts, which are spatially displaced (sheared) at the sample plane, and recombined before observation. However to produce the two orthogonal polarization quartz prism where used to illuminate the sample, in our proposed optical set-up both images are generated directly with two orthogonal polarization.

The paper is organized as follows: after this introduction, Section 2 introduces and described the optical setup and the main elements. Then, in Section 3 we present some experimental results on the application as different Fourier transform filters based on the phase-only modulation operation of the display. These results show how the microscope filter operates on axis. Then, section 4 introduces some other filtering operations based on the control of the state of polarization, which can be considered as a DIC equivalent. Finally, Section 5 present the conclusions of the work.

## 2. OPTICAL SYSTEM

The optical setup is shown in Fig. 1. A He-Ne laser ( $\lambda=633$  nm) is spatially filtered and collimated, and illuminates the sample. Then an infinity corrected microscope objective is used, a 10X objective from Nikon, with a focal length of  $f_{obj}=20$  mm. The Fourier transform (FT) of the sample transmittance is obtained in the back focal plane of the objective. However, it is difficult or even impossible to access this FT plane (FT plane 1 in Fig. 1). This, following previous systems [5,6], we use a relay optics composed of two converging lenses L1 and L2, with focal lengths  $f_1=175$  mm and  $f_2=400$  mm respectively, to image FT plane 1 onto FT plane 2, where the LCOS SLM can be placed. The relay optics can be viewed as a 4f system from FT plane 1 to FT plane 2. An intermediate image plane is produced in between (image plane 1). This magnification allows to have a FT size that can be manipulated with the LCOS SLM.

The LCOS SLM is used to display a diffractive mask that performs the Fourier transform filtering operation. Here we use a Hamamatsu LCOS display, parallel aligned PAL-LCOS-SLM model X10468-01, with 792×600 pixels, 20×20  $\mu\text{m}^2$  pixel size and video-rate operation (60 Hz). The LC director is oriented horizontal with respect to the laboratory frame. This device is a programmable linear retarder with the extraordinary axis oriented horizontally, and the ordinary axis oriented vertically. Therefore, it produces a phase-only modulation for linearly polarized light oriented horizontally. A phase retardation variation of  $2\pi$  radians is obtained for the operating wavelength of 633 nm for a gray level variation of 196 levels. The electronics of

the SLM is corrected to provide a linear relation of the retardance variation with the addressed gray level.

Light reflected back from the SLM is isolated from the input beam by means of a non-polarizing beam splitter (NPBS). A final converging lens (L3), with focal length  $f_3$ , performs a final FT operation. The final magnification of the microscope can be adjusted by adjusting the location of lens L3 and the CCD detector. We use a CCD camera from Basler, model sca1390-17fc, with 1392x1040 pixels.

Two rotatable polarizers are included in the system (P1 and P2), before and after the NPBS. The input polarizer (P1) is used to select the polarization of the beam impinging the LCOS SLM. Polarizer P2 is used to select the output transmitted polarization. The polarization of the beam illuminating the sample is selected circularly polarized, so polarizer P1 can be rotated without changing the intensity of the beam.

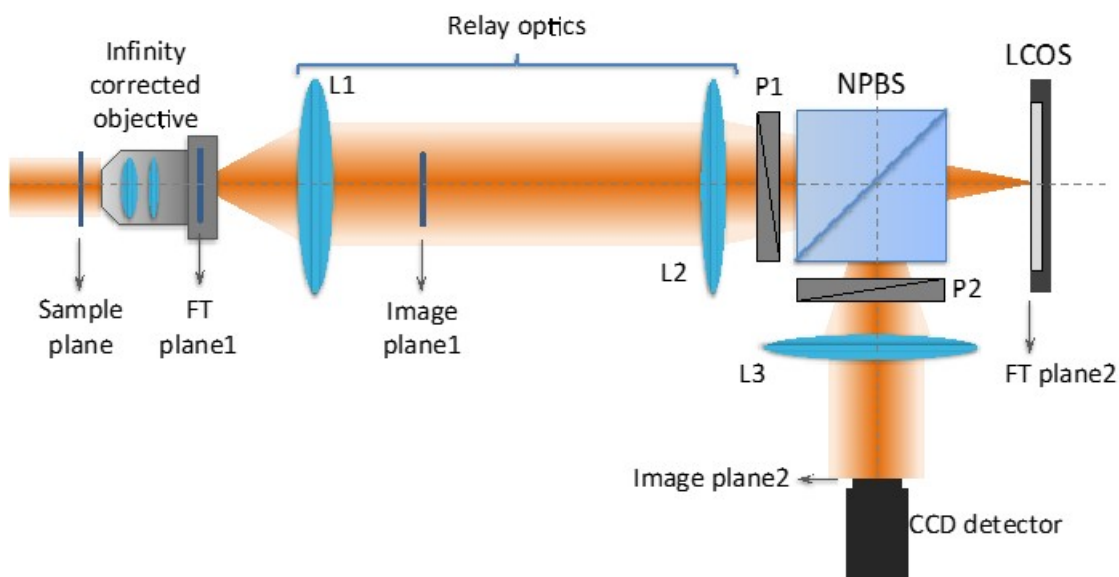


Fig. 1: Scheme of the optical setup. L denotes a converging lens, and P denotes a linear polarizer.

### 3. IMAGING PROCESSING OPERATIONS WITH PHASE-ONLY FILTERS

It is well known that by manipulating the spatial frequencies of the Fourier spectrum of an image different image processing operations such as band-pass filtering can be obtained [24]. For instance, high pass filtering produce edges detection whereas low pass filtering averages the borders by smoothing the image appearance. All those processes are normally applied to microscopic samples. However in a conventional microscope it is difficult to have access to Fourier plane where a mask should be placed in order to block the desired frequency band. It would be also complicated in a conventional microscope to apply different filters simultaneously.

Here we use the LCOS SLM to display blazed grating masks in the Fourier plane. For that purpose, we orient polarizers P1 and P2 horizontally, to be parallel to the LC director of the display, and this way produce a phase-only modulation operation. Then we have used a mask composed by a blazed grating acting in the high frequency domain, with the result of a first-diffraction order shifting of high frequency image, whereas a low-frequency image is obtained in the zero-order. The mask that we used is shown in Fig. 2(a). It consists on the central circle with uniform gray

level, surrounded with a blazed grating with 4 pixels period. The microscopic object is Microcopy Resolution Test Chart (NBS 1010A) test where number 18 is imaged. This is an amplitude resolution test is composed by five-bar chart. Each of the five bars in a test element is 25 times as long as it is wide. We have imaged number 18, meaning 8 cycles/mm, so the width of the number is around 65 microns.

The final image is shown in Fig. 2(b) corresponds to displaying constant image on the LCOS SLM, therefore not producing any filtering operation. The location of the number 18 image indicates the optical axis, since the object is selected centered. Note that there is no indication of a DC component that would appear if flickering were being produced in the SLM. Note also the sharp edges of the image.

Then, we apply the filter in Fig. 2(a) and the final image is placed in Fig. 2(c), and the result shows two version of the input object: 1) a low-pass filtered version of the object is obtained on axis, with smooth borders, corresponding to the low spatial frequencies passing through the circle with uniform gray level in Fig. 2(a); 2) a high-pass filtered edge enhanced version of the image is being obtained off axis, corresponding to the spatial frequencies being reflected on the outer part of the filter in Fig. 2(a), where the blazed grating diffracts the light with 100% efficiency onto the first diffraction order. One advantage of the system that is shown in Fig. 2(c) is that both high- and low-pass filtered images are obtained at once and simultaneously.

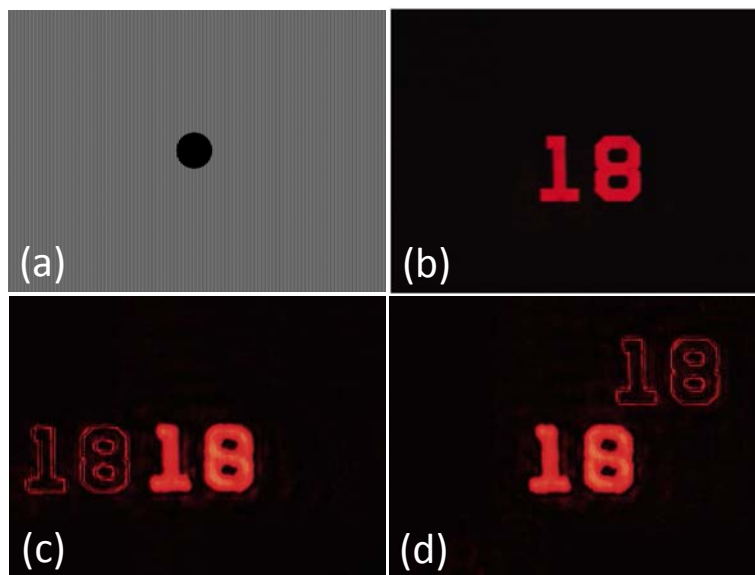


Figure 2. (a) Phase mask addressed on the LCD the Fourier plane, the blazed grating has a period of 4 pixels and the size of the circular mask has a radius of 45 pixels. (b) Image of number 18 in Microcopy Resolution Test Chart (NBS 1010A) (18 pairs/mm) using the microscope without filtering. (c) Final image plane with the two filtered images. (d) Equivalent results when the blazed grating is oriented at  $45^\circ$  with respect the LC director.

Note that by changing the orientation of the blazed grating, it is possible to direct the filtered first diffraction order onto different directions, as can be shown in Fig. 2(d), where the grating has been oriented at  $45^\circ$ , thus providing the high pass filtered version of the object to appear diffracted in the diagonal direction of the final image. The period of the grating can be adjusted as well, to provide different angular separation of the filtered image, and avoid overlapping with the opposite filtered image appearing on axis.

A similar experiment can be done but using now an opposite filter as provided by the phase mask in Fig 3(a), where the blazed grating is inside the central circle mask, and the surrounding image is uniform. In this case, the first diffracted order is the low-pass filtered version of the image, while the central image reproduces the high-pass version of the image. Again, changing the orientation of the blazed grating in the central circle allows changing the position of the low-pass image, while the high-pass filtered version is maintained in the original location (Figs. 3(b)-(d)).

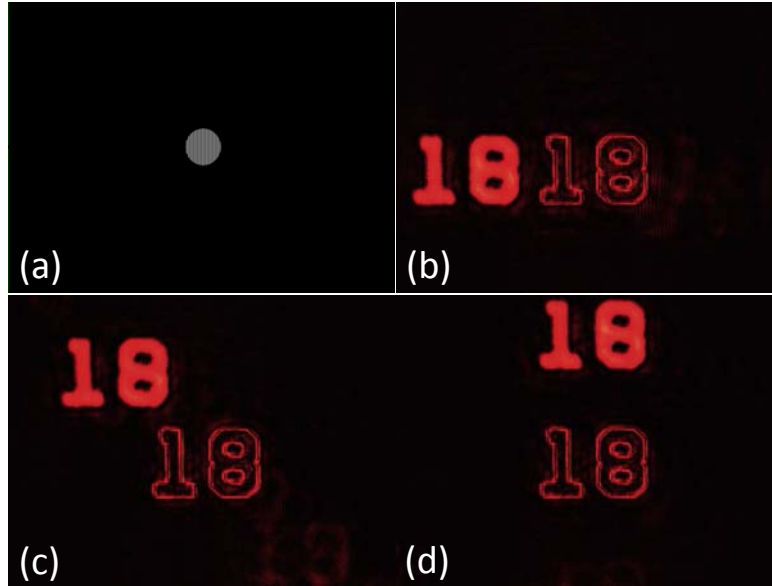


Figure 3. (a) Phase mask addressed on the LCD the Fourier plane, the blazed grating has a period of 4pixels and the size of the circular mask has a radius of 47 pixels. (b) Blazed grating oriented a 0°, (c) oriented at 135°, and (d) oriented at 90°.

These simple results demonstrate that the LCOS SLM is providing an excellent phase-only modulation, with no significant evidence of the zero order component of the diffraction grating, thus showing the full profit of the SLM space bandwidth. Nevertheless, the filtering operations require the use of a blazed grating to diffract off-axis the spatial frequencies that are filtered. Next we show that similar results can be obtained by exploiting of the polarization modulation provided by the display.

For the sake of clarity and in order to quantify our results, we have calculated the error of the high pass and low pass images in comparison to well-known digital image processing operation as Sobel and Gaussian filtering [24]. Sobel filtering is used as edge extractor simulating a high pass filtering whereas digital Gaussian filter smooth the borders acting as a low-pass filter. For simulating the digital results we have used a binary version of number 18 shown in Fig. 2(b). We have also select the same 1D profile of the images to make easier the comparison. The metric used to compare the 1D profiles of the images is the mean squared error (*MSE*) defined as:

$$MSE = \frac{1}{N} \sum_{n=1}^N [f_1(n) - f_2(n)]^2 \quad (1)$$

where  $f_1(n)$  and  $f_2(n)$  are respectively the 1D profile of the digitally filtered image, and the optical result obtained in our system, respectively and  $N$  is the number of pixels. We also calculated the Peak Signal-to-Noise Ratio (PSNR) defined as

$$PSNR = -10 \log_{10} \left( \frac{MSE}{S^2} \right) \quad (2)$$

where  $S$  is the maximum pixel value and the  $PSNR$  is measured in dB. We have normalized the images so  $S=1$ .

In Figure 4, we show a 1D profile of the filtered images to make easier the analysis.

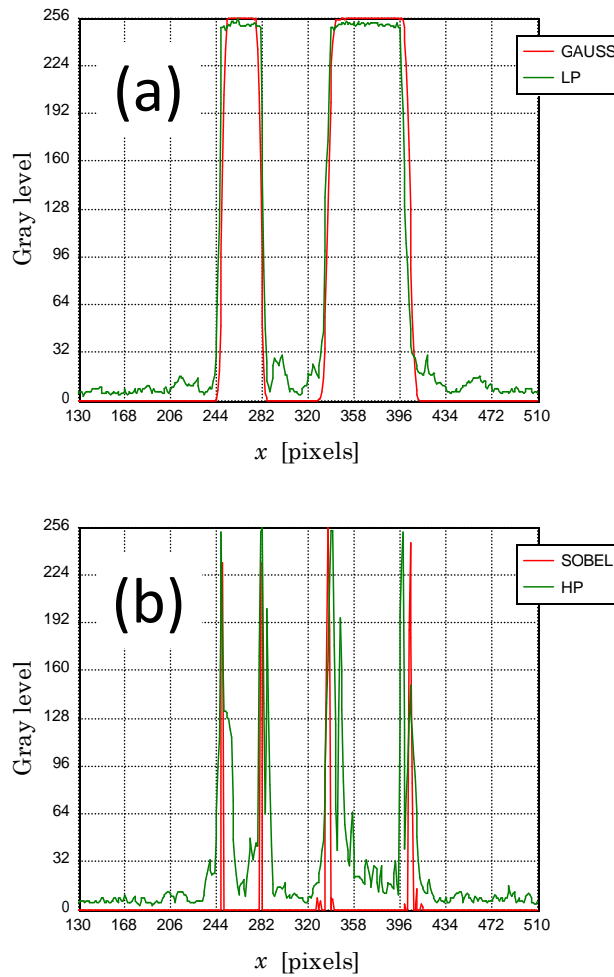


Figure 4. (a) 1D profile comparison for optical low pass image shown in Fig. 2 and 3, with (5x5 pixel window) digital Gaussian filter. (b) 1D profile comparison for optical high pass image shown in Fig 2 and 3 with (5x5 pixel window) digital Sobel filter.

In Fig. 4(a) we are comparing the 1D profile for digital Gaussian filter (in red) and our optical low-pass image (in green). The digital filter uses a window of 5x5 pixels. The MSE (in percentage) and PSNR for those profiles are 0.6% and 22.2dB, respectively. Note that the values show the good agreement between both profiles. In Fig. 4(b) we compare the 1D profile for digital Sobel filter

(in red) and our optical high-pass image (in green). Again the filter has a 5x5 pixels window. The MSE and PSNR are 2.6% and 15.8dB, respectively. For this case, the noise coming from experimental results is more evident, but still we have a good matching.

#### **4. IMAGING PROCESSING OPERATIONS USING POLARIZATION MODULATION**

Polarization is a degree of freedom widely used in microscopy. It is well known that biological samples and other materials exhibit changes in the polarization when they are illuminated. This optical property can be exploited to enhance the contrast in microscopy [26]. In our optical microscope we will be able to generate different final images with different polarizations by using the LCOS SLM as a polarization filter. For that purpose we follow the technique introduced in [27].

Previous results in Section 2 were obtained using the SLM as phase-only filter, and for that purpose the polarizers P1 and P2 were aligned both horizontal to be parallel to the LC director axis. However by selecting the polarizer P1 oriented at  $45^\circ$  angle with respect to the LC director and addressing a blazed grating in our SLM, two different beams are reflected with orthogonal polarizations. The horizontal polarization component, parallel to the LC director, is fully affected by the blazed grating and becomes 100% diffracted onto the first diffraction order. On the contrary, the vertical polarization component is completely unaffected by the mask displayed on the SLM, and it is reflected as if the display was a mirror.

As a consequence, if polarizer P2 is removed from the system, two images are obtained in the final plane with two orthogonal linear states of polarization. This result is shown in Fig. 5(a) where two equal images are obtained. Note that in this case the two images are identical, since no filtering operation is being performed yet (the blazed grating completely fills the SLM screen). But this duplication can be used for future image processing operation. To verify that both images have two different orthogonal polarization states we placed back the analyzer P2. In Fig 5(b) the analyzer is oriented vertical, i.e., perpendicular to the LC director of the LCOS-SLM. Therefore, only the zero order undiffracted image is recovered, and the off-axis shifted image is completely removed. On the contrary, when the analyzer P2 is oriented horizontal, i.e., parallel to the LC director, only the first-order image is obtained (see Fig. 5(c)), and the image on-axis is completely removed.



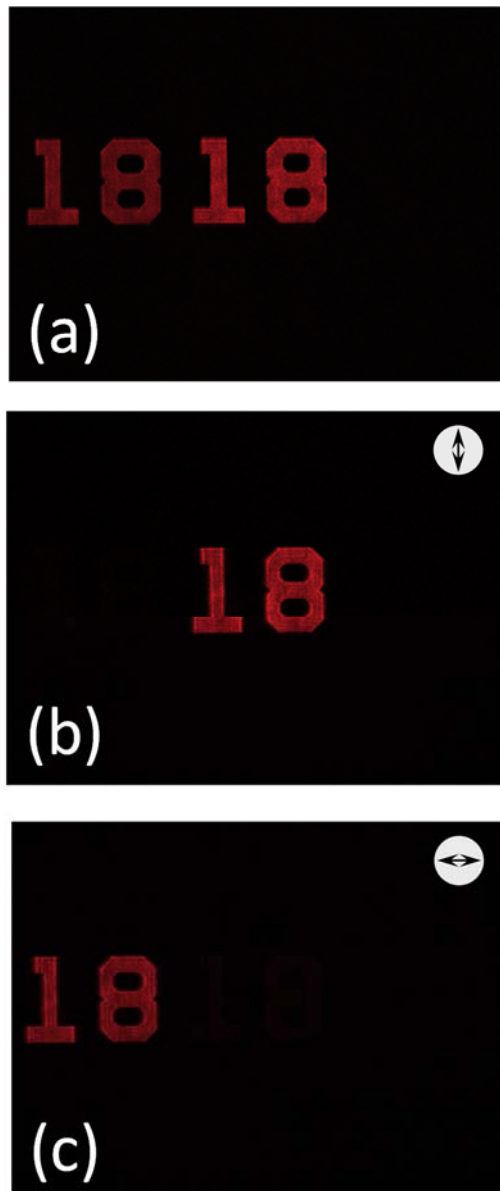


Figure 5. (a) Without analyzer, (b) Zero-order image, (c) First order image. The period of the blazed grating is 4 pixels. The orientation of the analyzer P2 is indicated on the top.

This result is relevant since we are not only obtaining duplicity of the images, but both images have different orthogonal linear polarization. Changing the period of the blazed grating we are able to change the relative lateral shift between both images. Therefore, we can reduce the diffraction angle of the blazed grating to make both images overlap, and then perform different basic imaging operations such addition and subtraction simply by rotating the analyzer P2.

As an example, in Figs. 6(a) and 6(b) we have implemented a blazed grating with a period of 7 pixels. Note that now the two images share a region where they overlap. In order to view both images with equal intensity we placed the analyzer P2 oriented at  $\pm 45^\circ$ . But the result is completely different depending on the sign. When P2 is oriented at  $+45^\circ$  with respect to the LC director, the linear polarizations of the two images project onto the analyzer axis with the same sense, and the images are added. On the contrary, when P2 is oriented at  $-45^\circ$ , the electric field

of the two images project with opposite sense, and a subtraction operation is produced. This is why the region of overlap appears bright in Fig. 6(a) and dark in Fig. 6(b). This addition and subtraction operation by means of polarization projection has been in fact used for years with magneto-optic modulators [28].

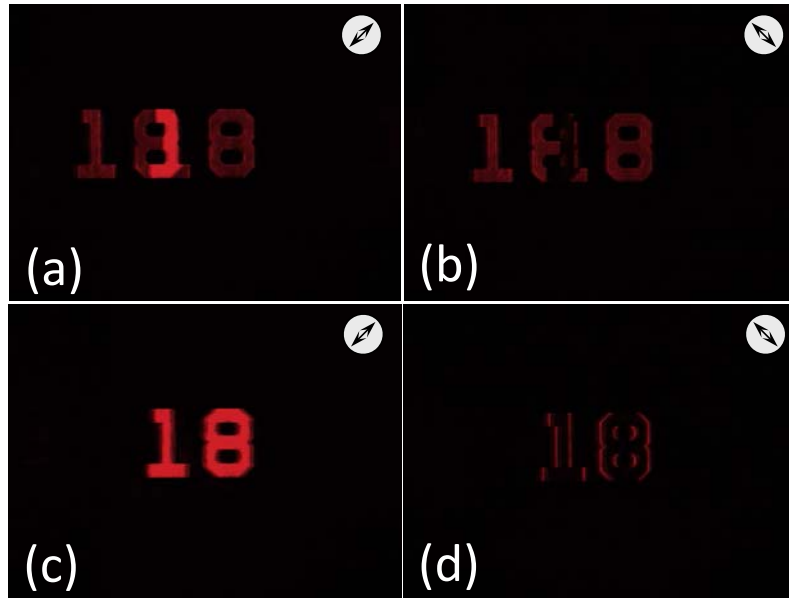


Figure 6. Addition and subtraction of the two images by means of polarization: (a)-(c) Analyzer P2 oriented at  $45^\circ$  to produce addition; (b)-(d) Analyzer P2 oriented at  $-45^\circ$  to produce subtraction. In (a)-(b) the blazed grating has a period of 7 pixels. In (c)-(d) the blazed grating has a period of 90 pixels.

This type of operation based on polarization allows reproducing the implementation of DIC type image processing. In fact DIC techniques use the interference of two beams to measure the path length difference between adjacent points in the image. It is like producing a gradient in the image. DIC works better in amplitude images since in typical biological samples the birefringence (phase content) is not too high and so the amplitude differences are not well visualized. Here we applied DIC to amplitude images. However DIC can be used to quantify phase and to obtained 3D profiles of the samples [12].

This is shown in Figs. 6(c) and 6(d). Here we have increased the period of the blazed grating to 90 pixels in order to reduce the angular diffraction and make the two images practically overlap. The small lateral displacement produces a high gradient of the final image. Therefore, when we orient the analyzer P2 at  $\pm 45^\circ$  to produce the addition and subtraction operations, we obtain a single version with smooth wedges (Fig. 6(c)) or enhanced edges (Fig. 6(d)). Note that these operations can be made on axis, exploiting the polarization orthogonally of the two beams because we use a LCOS-SLM without flicker effect. Otherwise, the on-axis zero-order component of the blazed diffraction grating will additionally contribute to the other polarization component, and prevent to perfectly produce these effects.

Note that the edge enhancement in Fig. 6(d) is produced only in the vertical edges, while the horizontal edges are not visible. This is due to the lateral displacement of the diffracted image, which is made in the horizontal direction in this example. This could be avoided for instance by implementing a diffractive lens on the LCOS-SLM instead of the blazed grating. If the focal length is large enough, the horizontal polarization will be focused in a plane slight different than the

vertical polarization, and will appear slightly defocused. Then the subtraction operation will provide all edges, as it was shown for instance in [29].

This is what we did in the final result provided in Fig. 7. Here we used as a sample a thin layer of onion skin cells. In order to avoid speckle due to the laser illumination, we incorporated a diffuser in the illumination of the sample. Figure 7(a) shows the images captured when the LCOS-SLM displays a uniform image. And Figure 7(b) shows results but now the SLM displays a diffractive lens of focal length as large as 2 meters and the analyzer P2 is oriented at  $-45^\circ$  to produce a subtraction of the focused and the defocused image. Now two images with orthogonal polarizations are again obtained, but instead of being laterally shifted, one of them is focused in the final plane, while the other one (affected by the diffracted lens on the SLM) is slightly defocused. This result in Fig. 7(b) reproduces the classical 3D effect characteristic of DIC imaging.

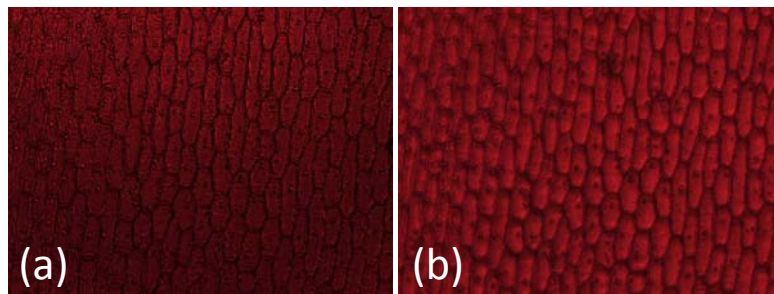


Figure 7. (a) Image of onion skin cells with uniform image in the SLM (b) 3D effect obtained by displaying a diffractive lens ( $f=2000$  mm) in the SLM.

Note that all these experiments included in this last section do not require to operating off-axis as other previous systems in the literature. Blazed gratings with very large period or lenses with very large focal length are implemented by the SLM, thus reducing the spatial resolution requirements in the display.

## 5. CONCLUSIONS

In summary, in this paper we have optically implemented a simple programmable microscope setup based on placing a LCOS-SLM in a Fourier transform plane, and we showed how it can perform different filtering operations. We have used a Hamamatsu LCOS-SLM free of flicker, which allows operating the system on axis, as opposed to other systems in the literature that must be operated off-axis due to the zero order component caused by this effect.

The possibility to modulate both the phase and the polarization of the optical beam permits to implement basic image processing operation for microscopic amplitude objects by selecting properly the polarization states. In addition we have implemented differential interference contrast (DIC) simply by generating two images exploiting the polarization splitting properties when a blazed diffraction grating is displayed in the SLM. This polarization based technique could be applied because of the operation on-axis achieved with the use of our LCOS-SLM display. Biological microscopy samples are used for enhancing contrast using a diffractive lens in the SLM.

In addition, due to the possibility to work on-axis, we can use the whole area of the SLM (800x600 pixels in our case) to codify the filtering masks. This is an advantage compared to other

systems in the literature, which must be operated off-axis due to the zero-order component, and therefore need to codify a grating to shift information to first-order.

## ACKNOWLEDGEMENTS

This research was supported Spanish Ministerio de Economía y Competitividad and FEDER Funds through grant FIS 2015-66328-C03-03

## REFERENCES

- [1] P. J. Smith, C. M. Taylor, A. J. Shaw, and E. M. McCabe, "Programmable array microscopy with a ferroelectric liquid-crystal spatial light modulator," *Appl. Opt.* **39**, 2664–2669 (2000).
- [2] W. J. Hossack, E. Theofanidou, J. Crain, K. Heggarty, M. Birch, "High-speed holographic optical tweezers using a ferroelectric liquid crystal microdisplay," *Opt. Express* **11**, 2053 (2003).
- [3] V. Nikolenko, B. O. Watson, R. Araya, A. Woodruff, D. S. Peterka, R. Yuste, "SLM microscopy: Scanless two-photon imaging and photostimulation with spatial light modulators", *Frontiers in Neural Circuits* **2**, 5 (2008).
- [4] M. A. A. Neil, T. Wilson, R. Juskaitis, "A wavefront generator for complex pupil function synthesis and point spread function engineering", *J. Microscopy* **197**, 219 (2000).
- [5] L. Camacho, V. Micó, Z. Zalevsky, and J. García, "Quantitative phase microscopy using defocusing by means of a spatial light modulator," *Opt. Express* **18**, 6755-6766 (2010).
- [6] C. Maurer, A. Jesacher, S. Bernet, and M. Ritsch-Marte, "What spatial light modulators can do for optical microscopy?," *Laser Photon. Rev.* **5**, 81–101 (2011).
- [7] M. Hasler, T. Haist, and W. Osten, "SLM-based microscopy," *Proc. SPIE* **8430**, 84300V (2012).
- [8] S. N. Khonina, V. V. Kotlyar, M. V. Shinkaryev, V. A. Soifer, and G. V. Uspleniev, "The phase rotor filter," *J. Mod. Opt.* **39**, 1147–1154 (1992).
- [9] J. A. Davis, D. E. McNamara, D. M. Cottrell, and J. Campos, "Image processing with the radial Hilbert transform: theory and experiments," *Opt. Lett.* **25**, 99–101 (2000).
- [10] S. FÜRhappter, A. Jesacher, S. Bernet, and M. Ritsch-Marte, "Spiral phase contrast imaging in microscopy," *Opt. Express* **13**, 689–694 (2005).
- [11] G. Popescu, *Quantitative phase imaging of cells and tissues*. New York: McGraw-Hill. (2011).
- [12] T. J. McIntyre, C. Maurer, S. Bernet, and M. Ritsch-Marte "Differential interference contrast imaging using a spatial light modulator," *Opt. Lett.* **34**, 2988-2990 (2009).
- [13] M. Warber, T. Haist, M. Hasler, W. Osten, "Vertical differential interference contrast", *Opt. Eng.* **51**, 013204 (2012).
- [14].A. Lizana, I. Moreno, A. Márquez, C. Lemmi, E. Fernández, J. Campos, and M. J. Yzuel, "Time fluctuations of the phase modulation in a liquid crystal on silicon display: characterization and effects in diffractive optics," *Opt. Express* **16**, 16711-16722 (2008)
- [15].Y. Calderón-Hermosillo, J. García-Márquez, R. Espinosa-Luna, N. A. Ochoa, V. López, A. Aguilar, E. Noé-Arias, Y. Alayli, "Flicker in a twisted nematic spatial light modulator," *Opt. Laser Eng.* **51**, 741-748 (2013).
- [16].J. Albero, P. García-Martínez, J. L. Martínez, I. Moreno, "Second order diffractive optical elements in a spatial light modulator with large phase dynamic range," *Opt. Lasers Eng.* **51**, 111–115 (2013).

- [17].J. L. Martínez, I. Moreno, M. M. Sánchez-López, A. Vargas, and P. García-Martínez, "Analysis of multiple internal reflections in a parallel aligned liquid crystal on silicon SLM," *Opt. Express* **22**, 25866-25879 (2014).
- [18].T. Colomb, F. Dürr, E. Cucho, P. Marquet, H. G. Limberger, R. P. Salathé, and C. Depeursinge, "Polarization microscopy by use of digital holography: Application to optical-fiber birefringence measurements," *Appl. Opt.* **44**, 4461-4469 (2005).
- [19].T. Oka and T. Kaneko, "Compact complete imaging polarimeter using birefringent wedge prisms," *Opt. Express* **11**, 1510-1519 (2003).
- [20].N. Hagen and M. W. Kudenow, "Review of snapshot spectral imaging technologies", *Opt. Eng.* **52**, 090901 (2013).
- [21].G. Normarski, "Interferometry with Schlieren microscopy", *J. Phys. Radium.* **16**, 9-11 (1955).
- [22].C. Preza, "Rotational-diversity phase estimation from differential –interference-contrast microscopy images," *J. Opt. Soc. Am. A* **17**, 415-424 (2000).
- [23].T. McIntyre, C. Maurer, S. Fassel, S. Khan, S. Bernet, and M. Ritsch-Marte, "Quantitative SLM-based differential interference contrast imaging," *Opt. Express* **18**, 14063-14078 (2010).
- [24].R. C. Gonzalez and R. E. Woods "Digital Image Processing", Third Edition, Prentice Hall (2007).
- [25].J.W. Goodman, *Introduction to Fourier Optics*, McGraw-Hill (1996)
- [26].V. V. Tukin, L. Wang and D. K. Zimnyakov "Optical polarization in biomedical applications" Springer (2013).
- [27].J. A. Davis, J. Adachi, C. R. Fernández-Pousa, I. Moreno, "Polarization beamsplitters using programmable polarization diffraction gratings," *Opt. Lett.* **26**, 587-589 (2001).
- [28].J. A. Davis and M. A. Waring, "Contrast ratio improvement for the two-dimensional magneto-optic spatial light modulator," *Appl. Opt.* **31**, 6183–6184 (1992).
- [29].J. A. Davis, G. H. Evans, K. Crabtree, I. Moreno, "Programmable birefringent lenses using a liquid crystal display," *Appl. Opt.* **43**, 6235-6241 (2004).